

Classification of Rubber Tree Leaf Diseases Using Multilayer Perceptron Neural Network

Noor Ezan Abdullah, Athirah A. Rahim, Hadzli Hashim and Mahanijah Md Kamal

Abstract-This paper presents about classification of rubber tree leaf diseases through automation and utilizing primary RGB color model. Several rubber tree leaf diseases are been studied for digital RGB color extraction where three sets of rubber tree leaf diseases image are digitally captured under standard and control environment. The identified regions of interest (ROI) of these diseases images are then processed to quantify the normalized indices from the RGB color distribution. This system involved the process of image classification by using artificial neural network where 600 samples were used as training while another 200 samples were for testing. The optimized ANN model in this work has two method which based only on the dominant pixel RGB (mean) and applying principle component analysis (PCA) on the pixel gradation values of each image. The optimized model was evaluated and validated through analysis of the performance indicators. Findings in this work have shown that both models have produced about 70% in diagnostic accuracy with more than 80% achievement for sensitivity. However, model with the applied PCA has lower network size.

Index Terms- RGB, Rubber Leaf Diseases, ANN, PCA

I. INTRODUCTION

Rubber is one of the most important products of Malaysia. Every year, large amount of latex are produced and due to the increasing of rubber-based products in the market, it is a necessity to maintain the quality and quantity. Thus, good care of the rubber tree must be taken so that they are free from diseases. The diseases of rubber can be divided into four categories; root, panel, stem and branch and leaf diseases [1]. Conventionally, prevention from diseases is through assessing via visual inspection regularly and tries to match its appearance to the closest appearance photo from a library text. However, this evaluation process are time consuming, has low percentage in accuracy and as well as costly [2].

Color perception plays important role in pattern recognition. It interacts with the surface and the interior of an object through absorption and scatterings. Thus, causes alteration in the spectral composition. Since color conveys significant information, color information seems to be suited as the first step in analyzing leaf disease [3]. Color space is commonly used for object recognition, color segmentation, image retrieval and image understanding. In color extraction,

color of a pixel is given as three values corresponding to the well known band R (Red), G (Green) and B (Blue) [4]. Other of color spaces are also used in color features extraction.

Artificial neural network (ANN) is basically a different paradigm for computing which are based on the processing of human information system. It is a form of multiprocessor computer system generally consists of simple processing data, high degree interconnection, simple scalar massages and adaptive interaction between elements [5]. ANN has been used for evaluating various pattern recognition or classifying purposes with various algorithms such as multi-layer back propagation, unimodal Gaussian, K- nearest neighbor, and nearest cluster algorithms [6].

With the advancement of computer technology, processing and analysis of any rubber leaves images can be visualized and can be very cost effective. Since leaves presentation can also be presented in terms of digital images, therefore they can be processed and measured to produce important quantitative features information. These features can be used then in designing an automated model for discriminating type of leaf disease. Therefore in this work, two models are proposed for automated disease identification using ANN Levenberg Marquardt. Model 1 (after this will be known as Ezan1) uses the three dominant pixel (mean) in RGB color space as the inputs, while Model 2 (after this will be known as Ezan2) utilizes only the input size of pixel gradation values for each image that has being reduced after applying principle component analysis (PCA). The optimized model is later evaluated and validated through analysis of the performance indicators.

II. METHODOLOGY

A. Data Collection

The leaf samples used in this research were collected from the nursery in Lembaga Getah Malaysia, Sg. Buloh. Three different classes of rubber trees were selected for this study which is the corynespora, bird's eye spot and collectotrichum. The leaf samples were collected from a number of different rubber trees that exhibited the various disease conditions. The samples were brought to a laboratory and then sealed in plastic bags with appropriate labels to maintain the moisture level of

the leaves. For this study, 700 of images have been collected where 300 images belongs to corynespora and 400 from the other two diseases. Figure 1 below shows samples of the three types of rubber tree leaf diseases. The proposed automated model is for classifying corynespora from bird's eye spot and collectotrichum because the later will effect the quantity of latex produced by the rubber tree.

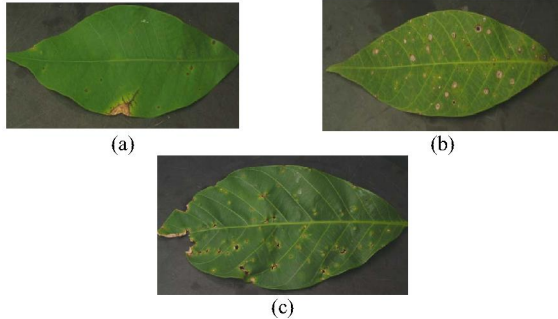


Figure 1: Types of Rubber Leaf Disease; (a) Corynespora, (b) Bird's Eye Spot and (c) Collectotrichum

B. Image Acquisition Procedures

The Red, Green, Blue (RGB) component color images were acquired using FinePix 6900 Zoom (Fuji Film) digital camera, with pixel resolution of 1280x960 and in form of JPEG format. This size is sufficient for analysis, as all relevant details of the lesions are shown [7]. The image capturing process was done at the Image Capturing Studio Room, located in the Advanced Signal Processing (ASP) Research Lab, Faculty of Electrical Engineering, UiTM Shah Alam. A detailed illustration of the image acquisition and classification process is given as shown in Figure 2 and 3 below.

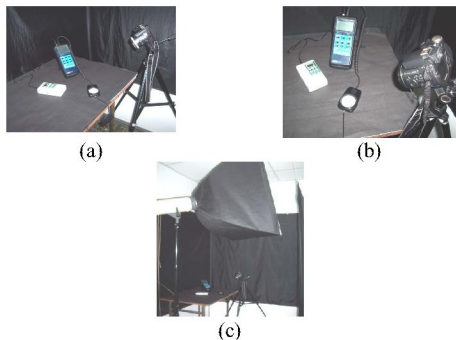


Figure 2: The image acquisition set – up; figure a-c shows the position of the equipment.

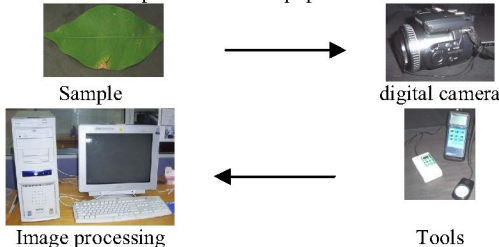


Figure 3: Image acquisition system

During the photo session, the camera was placed at a distance of one foot four inches directly above the rubber's leaf and the lighting source (Digi Color, K-250C, AC 170~

240V/50 Hz) angle is 80° from the sample. The light intensity was controlled by a standard lighting with mean lux of 130.6 ± 3.25 . the surrounding luminance was measured by using Heavy Duty Light Meter (Model 407026) interfaced with the Heavy Duty Data Logger (Model 380340). The image acquired has a dimension of 15 by 15 pixel area and data was recorded in pixel values of red, green and blue (RGB model).

C. Preprocessing

Conventionally, a color image of size $M \times N$ can be defined as 3 sequences of pixel level:-

$$r(m,n), \quad 1 \leq m \leq M ; 1 \leq n \leq N \quad (1)$$

$$g(m,n), \quad 1 \leq m \leq M ; 1 \leq n \leq N \quad (2)$$

$$b(m,n), \quad 1 \leq m \leq M ; 1 \leq n \leq N \quad (3)$$

where each element pixel representing R, G and B component respectively [8]. The individual color components are typically represented by 8-bit which means that each element would be an integer in the interval [0,255]. In any processing of 8-bit images, the integer restriction is abandoned and the image is processed in a floating point representation in order to minimize quantization effects.

D. Median Filtering

The first step in the process was the preprocessing of images with the purpose of reducing noise and facilitating image segmentation by using median filtering. The imaging technique may be noisy in terms of small white ellipse lines or dots. This artifact can be considered as impulsive noise and may thus be reduced using a median filter given by:

$$P_{med}(m,n) = median\{P(m-k, n-1) | -\frac{N_{med}-1}{2} \leq k, \\ l \leq \frac{N_{med}-1}{2} \wedge 1 \leq m-k \leq m \wedge 1 \leq n-1 \leq N\} \quad (4)$$

where N_{med} is odd² and indicates the size of the two dimensional median filter. P represents all the three color components and only square median filter kernel was considered [9].

E. Learning Rule

There are two types of learning rule; supervised and unsupervised learning to train the network. The former rule is provided with a set of examples (the training set) of proper network behavior and acts as the input to the network to achieve the corresponding correct (target) output. As the inputs are applied to the network, this type of learning rule is then used to adjust the weights and biases of the network in order to move the network output closer to the targets. While the latter learning rule, the weights and biases are modified in responses to network inputs only. There are no target outputs available.

F. Lavenberg – Marquardt Algorithm.

Like the quasi-Newton methods, the Levenberg-Marquardt algorithm was designed to approach second-order training speed without having to compute the Hessian matrix. When the performance function has the form of a sum of squares (as is typical in training feed forward networks), then the Hessian matrix can be approximated as,

$$H = J^T J \quad (5)$$

And the gradient can be computed as

$$g = J^T e \quad (6)$$

Where J is the Jacobian matrix, which contains first derivatives of the network errors with respect to the weights and biases, and e is a vector of network errors. The Jacobian matrix can be computed through a standard back propagation technique that is much less complex than computing the Hessian matrix. The Levenberg-Marquardt algorithm uses this approximation to the Hessian matrix in the following Newton-like update:

$$X_{k+1} = X_k J^T - [J + mI]^{-1} J^T e \quad (7)$$

When the scalar m is zero, this is just Newton's method, using the approximate Hessian matrix. When m is large, this becomes gradient descent with a small step size. Newton's method is faster and more accurate near an error minimum, so the aim is to shift towards Newton's method as quickly as possible. Thus, m is decreased after each successful step (reduction in performance function) and is increased only when a tentative step would increase the performance function. In this way, the performance function will always be reduced at each iteration of the algorithm [10].

G. Principal Component Analysis (PCA)

In some situations, the dimension of input vector is large with redundancy in its component values. Thus, it is useful to reduce the input dimension size. An effective procedure for performing this operation is the principal component analysis. This technique has three effects: it orthogonalizes the components of the input vectors (so that they are uncorrelated with each other); it orders the resulting orthogonal components (principal components) so that those with the largest variation come first; and it eliminates those components that contribute the least to the variation in the data set [11].

H. Designing of ANN Pattern Classifier

The main objective in this research is to discriminate corynespora from other diseases. Since it is also necessary to classify the diseases into a discrete category, feed forward neural networks were ideally suited for such purpose. The type of network that best fits in the diagnosis application is the multilayered perceptron (MLP) network with one hidden layer based on the fact that it has been widely satisfactorily applied by many researchers. The network is shown in Figure 4 and the output can be expressed by the following equations:

$$\hat{y}_i = \sum_{j=1}^t w_{ij}^2 f \left\{ \sum_{k=1}^s w_{jk}^1 x_k^0 + b_j \right\} \quad (8)$$

where $i = 1$ and w_{ij}^2, w_{jk}^1, b_j denotes the adaptive variables to be optimized and their values are changed many times during the network training process. The $f(\bullet)$, is the sigmoidal linear activation function which was used to map the sum of the weighted inputs to the output of a neuron in the hidden layer. The network was trained with supervision using a gradient descent training technique (also called as generalization of the delta rule or back propagation algorithm [12]), which minimizes the sum-squared error between actual output of the network and the desired output as:

$$J = \frac{1}{2} \sum_i (y_i - \hat{y}_i)^2 \quad (9)$$

where y_i and \hat{y}_i is the desired and calculated output produced by the ANN.

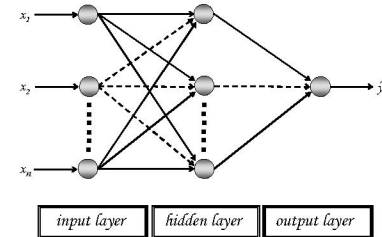


Figure 4: Architecture of the network model

Sensitivity and specificity are commonly used terms that generally describe the accuracy of a test. Sensitivity is a measure of the ratio or percentage of 'true' disease (TP) and a positive diagnostic test result ($D+$). It represents the actual percentage of a 'true' disease realized by a positive test result and is also known as true positive rate (TPR), defined as:

$$\text{Sensitivity: } TPR = \frac{TP}{D+} \quad (10)$$

Specificity measures the ratio or percentage of 'false' disease (TN) and with a negative diagnostic test result ($D-$). It is actually represents the actual percentage of a 'false' disease condition realized by a negative diagnostic test. Specificity is also termed as true negative rate (TNR) and is given as:

$$\text{Specificity: } TNR = \frac{TN}{D-} \quad (11)$$

The percentage for diagnostic accuracy (DA) refers to the percentage of samples that have been correctly classified or diagnosed, and have output values within the predefined threshold range for the respective output level. It can be derived as:

$$DA = \frac{\sum_{i=1}^N c_i}{N} \times 100\% \quad (12)$$

Variable c_i serves as counter for the proposed ANN model output, y at sample i . c_i is defined as:

$$c_i = \begin{cases} 1, & 1-thr \leq y \leq 1+thr \quad \text{for true} \\ 1, & -1-thr \leq y \leq -1+thr \quad \text{for false} \\ 0, & elsewhere \end{cases} \quad (13)$$

At each experiment, the respective number of neurons in the hidden layer was optimized based on the performance evaluation of the model through the sum-squared error (SSE) analysis as well the diagnostic accuracy (DA). At a later stage, the most appropriate threshold level would be decided by analyzing the minimum *Euclidean Distance* (ED) values from the receiver operating characteristic (ROC) plot [13].

III. RESULT AND DISCUSSION

A. Sample Size Reduction by using PCA

In this experiment, model Ezan2 is using the PCA algorithm to reduce the samples size of the pixel data. Throughout this project, PCA is set to retain 98% of the original variability of the data. Application of the sample PCA reduction has reduces the input from 675 to 2, which are displayed in Figure 5. The figure displays 400 samples data for corynespora and followed by from 200 for non-corynespora (bird's eye spot and collectotrichum). It can be observed significantly that corynespora can be discriminated from other diseases. Thus, training of the ANN model would be easier then.

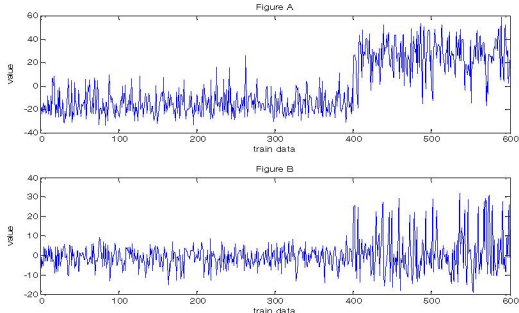


Figure 5: The first (A) and second (B) components of training data after the sample size reduction by PCA

B. Comparisons of the Performance Indicator

Since in this experiment, the primary focus for training is to distinguish corynespora from other diseases, between 50% - 75% of the training and testing gradation indices were obtained from corynespora category. Specially, the color gradation indices ratio distribution of the corynespora, bird's eye spot and collectotrichum used in the training and testing sets were 400:100:100 and 100:50:50 respectively. Thus the ratio between corynespora and non-corynespora for training was fixed at 400:200 and for testing was 100:100.

Figure 6 shows the performance of 5 best selected hidden layer size; 5, 7, 10, 13 and 15. It is shown that SSE performance converges for each model as it approaches to 1000 epochs. This implies that the training of the models is successful for each experiment.

After training, the network was tested with the testing data set. The performance plot for model Ezan1 is shown in Figure 7 in terms of sensitivity, specificity, and accuracy. Outcomes from these figures have shown that the optimized model utilized 5 neurons in its hidden layer. The model's accuracy achievement has reached 96.5%.

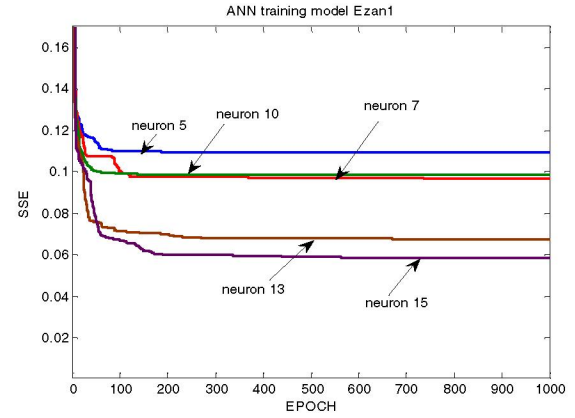


Figure 6: ANN RGB Model Ezan1 (SSE training performance)

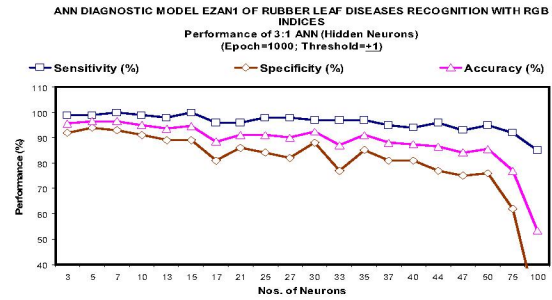


Figure 7: ANN RGB Model Ezan1 shows the performance of hidden layer size. Model with 5 neurons is selected because of having the highest accuracy (96.5%). Over-fitting occurs when the number of neurons is increased.

The following performance plots (Figure 8 and Figure 9) shown are for the second model constructed (Ezan2). Figure 8 shows the performance of 5 best hidden layer size; 5, 7, 10, 13 and 21. SSE performances are detected to be converged for each model as it approaches to 1000 epochs. Thus, the training is successful.

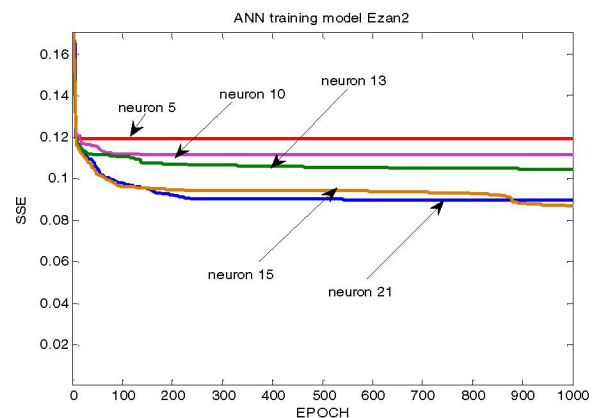


Figure 8: ANN RGB Model Ezan2 (SSE training performance)

Figure 9 shows performance plot for second neural network model Ezan2. From the experiment, the optimized model utilized 5 neurons in its hidden layer. The model's accuracy achievement has reached 96.5%.

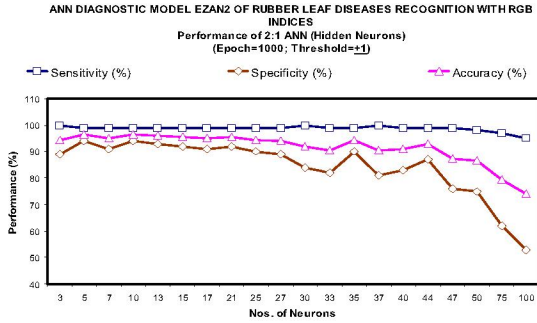


Figure 9: ANN RGB Model Ezan2 shows the performance of hidden layer size. Model with 5 neurons is selected because of having the highest accuracy (96.5%). Over-fitting occurs when the number of neurons is increased.

Additional information can be deduced from comparison of the available model. Figure 10 shows the ROC curve for each diagnostic model for Ezan1 and Ezan2. These figures also explain the nearest point of each curve to the ideal point (0, 1). The point with minimum Euclidean Distance (*ED*) for model Ezan1 is at threshold 0.4 while the *ED* point for model Ezan2 is at threshold 0.7. Nearer to this ideal point means shorter *ED* where it indicates better sensitivity and specificity of the ANN model. From the Figure 10, the total area under curve with respect to the labeled threshold is calculated as:

$$\begin{aligned} AUC_{Ezan1} &= 99\% \\ AUC_{Ezan2} &= 98\% \end{aligned}$$

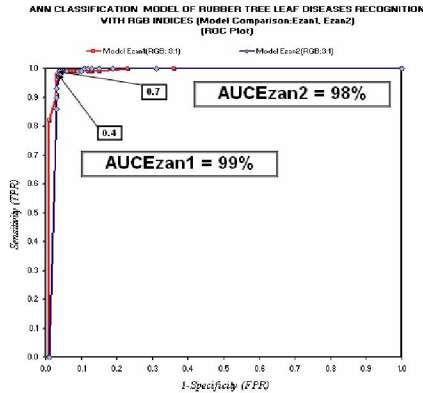


Figure 10: Comparison of ROC plots between Ezan1 and Ezan2

The area under both systems is almost equal implying both systems have good classification accuracies, indicated by [14]:

- a. Both curves leaning very closely to the upper left corner of the plot, and far from the diagonal line.
- b. The areas under the curve are very close to 100%, indicating very good specificity and sensitivity scores

Scatter plot is drawn to determine the closeness between the expected values and the ANN outputs. The scatter plot for model Ezan1 and model Ezan2 are shown in the Figure 11. Both figures have shown that, clustering is condensed at each true and false level.

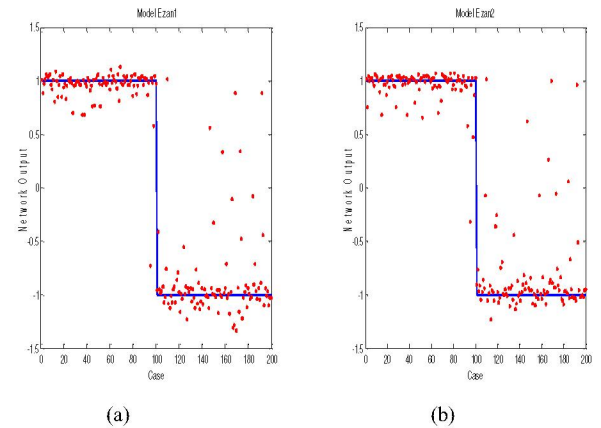


Figure 11: Scatter plot of (a) Ezan1 and (b) Ezan2. The solid line represent the expected output, the dots represent the network-simulated output.

A threshold (*thr*) is defined in order to examine the clustering power of network outputs at the different threshold. The effect of threshold adjustment is shown in Figure 12.

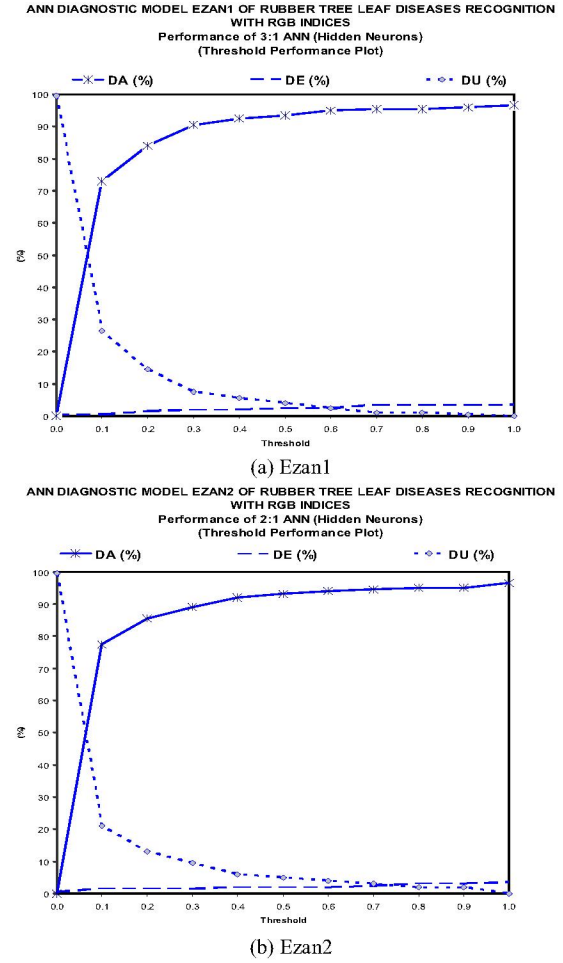


Figure 12: Effect of threshold on classification properties

The figure shows that Ezan1 has retained 92.5% DA for *thr*=0.4 while for Ezan2 at 94.5% DA for *thr*=0.7. Both systems exhibit low diagnostic error (DE) and diagnostic uncertainty (DU) which is below 10% at these thresholds. However, by comparing both model at *thr* = 0.1, Ezan2's DU have lower uncertainty rates (21%) and higher DA (77.5%)

compared to Ezan1 ($DU = 26.5\%$ and $DA = 73\%$). The outcome indicates that, there is slight different of diagnostic rates between both model at $thr = 0.4$ and $thr = 0.7$ respectively, if compared when the threshold is fixed at $thr = 0.1$. Thus, the later threshold is recommended to be used for classification. With respect to this threshold, Ezan2 has shown better performance than Ezan1 due to its good diagnostic rates.

Table 1 depicts the summarization of the necessary performance indicator for the available models. From the table, it is shown that at threshold (thr) 0.1, both models have same performance of hidden layer size and slightly equal value of AUC. However, model Ezan2 has better performance of sensitivity, specificity and DA than model Ezan1. In addition, model Ezan2 has smaller network size than Ezan1 and as well as having good diagnostic rates at this threshold.

Table 1: Overall performance between model Ezan1 and Ezan2.

Comparison between Models		
Model	Ezan1	Ezan2
Color	RGB	RGB
Method	RGB_{mean}	RGB_{PCA}
Threshold	0.1	0.1
ANN (Input:Hidden:Output)	3:5:1	2:5:1
ANN (No. of connections)	24	18
Sensitivity (%)	82	86
Specificity (%)	64	69
DA (%)	73	77.50
AUC (%)	99	98

IV. CONCLUSION

This research mainly presents a contribution in the field of color image processing of selected leaf diseases for rubber tree industry. RGB color variations and variegations are useful features used to discriminate between diseases. The extracted RGB color indices are then used to produce intelligent model system for rubber leaf diseases classification. The optimized ANN models designed in this research were based on the dominant pixel (mean) RGB known as Ezan1 and normalized PCA data of RGB components known as Ezan2. The optimized models were then evaluated and validated through analysis of the performance indicators.

Overall, both models (Ezan1 and Ezan2) able to achieve near 100% classification where the best accuracy is 96.5%, while sensitivity and specificity has achieved to more than 90%. In addition, the area under curve for both models are also slightly equal (99% for Ezan1, 98% for Ezan2). From the ROC plots, each model have different set of best threshold (0.4 and 0.7 respectively) calculated in terms of Euclidean distance from the ideal point at the top left hand corner. However, after analyzing the clustering power plots at threshold of 0.1, it is found that, Ezan2 is the best model since it produced better accuracy. Moreover, Ezan2 consumed small network size compared to Ezan1, thus reducing manufacturing cost. Therefore, this model can be concluded as the best model

for intelligent diagnostic for classifying corynespora from bird's eye spot and collectotrichum.

V. FUTURE RECOMMENDATION

In order to increase the effectiveness of this classification system, it is recommended to use a high pixel of digital camera for higher accuracy of capturing color images and providing better processor and computer specifications since the color resolution and processing time totally relies on the processor used. In addition, other color models can also be explored and included at the input for better efficiency in the training of the intelligent model. Besides that, other types of rubber tree leaf diseases such as fusicoccum and powdery mildew can be used as samples for this study.

VI. ACKNOWLEDGEMENT

The author would like to acknowledge the project supervisor, Assoc. Prof. Dr Hadzli Hashim for his encouragement and suggestions. Also, thankfulness to Dr. Masahuling Benong, Head of Crop Improvement and Protection Unit and Miss Murnita, Researcher Officer, both from Rubber Research Institute of Malaysia (RRIM), for their willingness to share their knowledge as well as providing the materials that has made this work excitably fruitful.

VII. REFERENCES

- [1] Rao.B.Sripathi, *Maladies of Hevea in Malaysia*, 1975.
- [2] B. S. Anami, D.G.Savakar, A. Makandar, and P. H. Unki, "A Neural Network Model for Classification of Bulk Grain Samples Based on Color and Texture," presented at Proceedings of the International Conference on Cognition and Recognition.
- [3] M. S. Baharudin, "Color Models Quantification of Skin Lesion using MATLAB GUI," Universiti Teknologi MARA, Shah Alam, Malaysia, 2006.
- [4] H.Hashim, R. A. Rahman, R.Jarmin, and M.N.Taib, "A Study on RGB color Extraction of Psoriasis Lesion using Principle Component Analysis (PCA)," presented at Student Conference on Research and Development (SCOReD2006), Shah Alam, Malaysia, 2006.
- [5] R.Pydipati, T.F.Burks, and W. S. Lee, "Statistical and Neural Network Classifier for Citrus Disease Detection Using Machine Vision," *Transaction of the ASAE*, vol. 48(5), pp. 2007-2014, 2005.
- [6] Miller, W.M, J. A. Throop, and B.L.Upchurch, "Pattern recognition models for spectral reflectance evaluation of apple blemishes.," *Postharvest Biology and Tech.*, vol. 14(1), pp. 11-20, 1998.
- [7] A.Bittorf, M.Fartsch, G.Schuler, and T.L.Diepgen, "Resolution Requirements for Digital Images in Dermatology," *Journal American Academy Dermatology*, vol. vol. 37, pp. 195-198, 1997.
- [8] A.K.Jain, *Fundamentals of Digital Image Processing*: Prentice Hall, 1989.
- [9] M.Sonka, V.Hlavac, and R.Boyle, *Image Processing . Analysis and Machine Vision*. London: Chapman Hall, 1993.
- [10] MATLAB, "Lavenberg Marquardt," in *Matlabs 7.0 Help*, 2007.
- [11] MATLAB, "Principle Component Analysis," in *Matlabs Help*, 2007.
- [12] S. Haykin, "Multilayer Perceptrons and Radial-Basis Function Networks," in *Neural Network*. New York: Macmillan College Publishing Company, 1994, pp. 138-281.
- [13] B.O'Connel and H.Myers, "Receiver Operating Characteristic (ROC) curves," *Journal of Clinical Nursing*, vol. 11, pp. 134-136, 2002.
- [14] I. M. Yassin and M. N. Taib, "Particle Swarm Optimization as Network Optimizer for Neural Network Based Face Detector," *IEEE*.